AGU PUBLICATIONS

JGR

Journal of Geophysical Research: Space Physics

RESEARCH ARTICLE
10.1002/2017JA024196

Key Points:
- We report the first extraterrestrial observations of Spontaneous Hot Flow Anomalies (SHFAs) in the foreshocks of Venus and Mars
- Although occurring at different planets, the events were very similar in duration and character
- SHFAs have the capability to directly impart energy into the ionospheres of unmagnetized planets

Correspondence to:
G. Collinson,
glyn.a.collinson@nasa.gov

Citation:
Collinson, G., et al. (2017), Spontaneous hot flow anomalies at Mars and Venus, *J. Geophys. Res. Space Physics*, *122*, doi:10.1002/2017JA024196.

Received 28 MAR 2017
Accepted 12 AUG 2017
Accepted article online 21 AUG 2017

Spontaneous hot flow anomalies at Mars and Venus

Glyn Collinson[1,2,3], David Sibeck[1], Nick Omidi[4], Joseph Grebowsky[1], Jasper Halekas[5], David Mitchell[6], Jared Espley[1], Tielong Zhang[7], Moa Persson[8], Yoshifumi Futaana[8], and Bruce Jakosky[9]

[1]NASA Goddard Spaceflight Center, Greenbelt, Maryland, USA, [2]Institute for Astrophysics and Computational Sciences, The Catholic University of America, Washington, District of Columbia, USA, [3]Interplanetary Expeditions, Berkeley, California, USA, [4]Solana Scientific, Solana Beach, California, USA, [5]Department of Physics and Astronomy, University of Iowa, Iowa City, Iowa, USA, [6]Space Sciences Laboratory, University of California, Berkeley, California, USA, [7]Space Research Institute, Austrian Academy of Sciences, Graz, Austria, [8]Institutet för rymdfysik, Swedish Institute of Space Physics, Kiruna, Sweden, [9]Laboratory for Atmospheric and Space Physics, Boulder, Colorado, USA

Abstract We report the first observations of Spontaneous Hot Flow Anomalies (SHFAs) at Venus and Mars, demonstrating their existence in the foreshocks of other planets beyond Earth. Using data from the ESA *Venus Express* and the NASA *Mars Atmosphere and Volatile EvolutioN (MAVEN)* spacecraft, we present magnetic and plasma observations from events at both planets, exhibiting properties similar to "classical" Hot Flow Anomalies, with bounding shock-like compressive regions and a hot and diffuse core. However, these explosive foreshock transients were observed without any attendant interplanetary magnetic field discontinuity, consistent with SHFAs observed at Earth and our hybrid simulations.

1. Introduction

Upstream from any celestial body lies a turbulent region in magnetic connection to the bow shock known as the foreshock [*Asbridge et al.*, 1968; *Greenstadt et al.*, 1968] (also see *Eastwood et al.* [2005] for a review of Earth's foreshock). Exploration of Earth's foreshock has revealed it to be home to a plethora of transient energetic particle and wave phenomena. Despite lasting for only a few minutes, these foreshock transients are important at the Earth because they can have dramatic global effects on the entire magnetosphere and even on the ionosphere [*Sibeck et al.*, 1998, 1999; *Eastwood et al.*, 2008]. Foreshock transients are therefore a fundamental mode of interaction between the solar wind and the Earth, and one suspects this to be true at other planets in the solar system.

Perhaps, the best known type of foreshock transient is the Hot Flow Anomaly (HFA). HFAs are explosively expanding bubbles of hot tenuous plasma which form when certain discontinuities in the interplanetary magnetic field (IMF) interact with a planetary bow shock [*Thomsen et al.*, 1993; *Schwartz*, 1995; *Schwartz et al.*, 2000]. Solar wind particles, reflected from the bow shock, can be swept toward the interplanetary current sheet where they become trapped and heated when the motional electric fields have the appropriate orientation. The result is a hot core of strongly deflected plasma with bulk velocities much slower than those of the solar wind, in which the magnetic field drops precipitously in magnitude and displays significant fluctuations [*Tjulin et al.*, 2008; *Kovacs et al.*, 2014]. This hot core is bounded by strong compression regions with denser and hotter plasma and enhanced magnetic field strengths. These events, which occur at Earth at a rate of about one per day [*Schwartz et al.*, 2000], have been studied extensively at Earth by missions such as *Interball* [*Vaisberg et al.*, 1999], *Cluster* [*Facskó et al.*, 2009; *Lucek et al.*, 2004], and *Time History of Events and Macroscale Interactions during Substorms* (*THEMIS*) [*Eastwood et al.*, 2008; *Zhang et al.*, 2010]. HFAs are thought to be a universal phenomenon, having been observed at Mars [*Øieroset et al.*, 2001; *Collinson et al.*, 2015], Saturn [*Masters et al.*, 2008, 2009], Venus [*Slavin et al.*, 2009; *Collinson et al.*, 2012a, 2014], and Mercury [*Uritsky et al.*, 2014]. In this paper, this type of foreshock transient which requires an IMF discontinuity for its formation shall be referred to as a "classic" HFA, or simply an HFA.

Recently, a new class of explosive foreshock transient has been identified upstream of Earth in both *THEMIS* observations by *Zhang et al.* [2013] and hybrid simulations by *Omidi et al.* [2013]. These phenomena bear all

the known characteristics of a classic HFA, but curiously, are not associated with any IMF discontinuity, thought to be so critical for classic HFA formation. Given their apparent proclivity for forming without any apparent external impetus, the phenomena were termed "*Spontaneous* Hot Flow Anomalies" (or SHFA). Hybrid simulations [*Omidi et al.*, 2013] confirmed that whilst very similar in characteristics to classical HFAs, SHFAs form in Earth's foreshock through an entirely different mechanism (to be outlined shortly) without the need for an IMF discontinuity, and thus whilst bearing a similar name and appearance, are in fact a wholly separate phenomena.

To date, SHFAs have only been reported in Earth's foreshock. Whilst the unmagnetized inner planets of Mars and Venus are known to have foreshocks, relatively little is known about what energetic transient phenomena may be encountered therein. In this paper, we present magnetic, electron, and ion measurements of explosive Spontaneous Hot Flow Anomalies encountered at Mars by the NASA *Mars Atmosphere and Volatile EvolutioN (MAVEN)* (2014 to present) and at Venus by the European Space Agency (ESA) *Venus Express* (2006–2014).

This paper is arranged as follows. In section 2, we review the induced magnetospheres and foreshocks of Mars and Venus, outline the formation mechanisms for SHFAs at Earth, and present a brief summary of preliminary results of new hybrid simulations predicting their formation at these planets through similar means (see companion paper *Omidi et al.* [2017] for full details). In section 3 we present a case study of a Martian SHFA observed on 7 January 2016 by *MAVEN*. In section 4 we present a case study of a Venusian SHFA observed on 18 October by the *Venus Express*. In section 5 we discuss the properties of the SHFAs and speculate what effects an SHFA might have on the unmagnetized planets of Mars and Venus. Finally, in section 6 we summarize our findings.

2. Assessment of SHFA Formation Conditions at Mars and Venus

2.1. The Induced Magnetospheres of Venus and Mars

Although Mars and Venus have no intrinsic global magnetic field [*Smith et al.*, 1965a, 1965b], their conductive ionospheres create a barrier to the solar wind. Interplanetary magnetic field (IMF) lines frozen into the solar wind flow collide with the planetary ionosphere and pile up on the dayside, resulting in the generation of an induced magnetosphere. This induced magnetic field is an obstacle to the supersonic solar wind and thus a supersonic bow shock is generated [*Ness et al.*, 1974; *Russell et al.*, 1979], just as with Earth's magnetosphere. However, the resulting solar wind obstacles are considerably smaller than Earth's. In order to cross the terrestrial bow shock at its closest distance (at the subsolar point), one would have to travel to a distance of ≈15 Earth Radii [*Fairfield*, 1971] from Earth's center (where $1R_E = 6371$ km), whereas Venus' subsolar bow shock lies at a distance of only ≈1.38 Venus Radii [*Slavin et al.*, 1980] ($1R_V = 6052$ km) from Venus' center, and Mars' bow shock is even smaller in absolute dimensions, at ≈1.6 Martian Radii [*Vignes et al.*, 2000] ($1\ R_M = 3390$ km).

Despite the relatively diminutive size of the Venusian and Martian bow shocks both generate foreshocks, although they are similarly miniature with respect to Earth's, with Venus' foreshock only extending 15 R_V upstream from the bow shock [*Strangeway and Crawford*, 1995]. Figure 1a shows a sketch of the expected topology of the Martian and Venusian induced magnetospheres and foreshocks (based on a hybrid code simulation to be described in brief shortly, and in detail in a companion paper [*Omidi et al.*, 2016], and the formation of an SHFA).

In this paper, we shall universally use the comparable planet-centric Venus Solar Orbital (VSO) and Mars Solar Orbital (MSO) coordinate systems, where x points toward the Sun, y points back along the tangent to the orbit of the planet around the Sun, and z completes the right-handed set, pointing upward out of the plane of the ecliptic (in this way, VSO and MSO are the Venusian and Martian equivalents to the terrestrial "GSE" coordinate system). For the purposes of the example sketch shown in Figure 1a, we have chosen to make the interplanetary magnetic field "radial," which is to say that it is dominated by the B_x component, lying parallel to the Sun-Planet line. However, SHFAs are known to form under at all angles of the IMF at Earth [*Omidi et al.*, 2014].

2.2. SHFA Formation

The foreshock of any celestial body is pervaded by a field of ultra-low frequency (ULF) waves [*Fairfield*, 1969; *Scarf et al.*, 1970] (see Figure 1) which are thought to be driven by field-aligned ion beams reflected at the bow

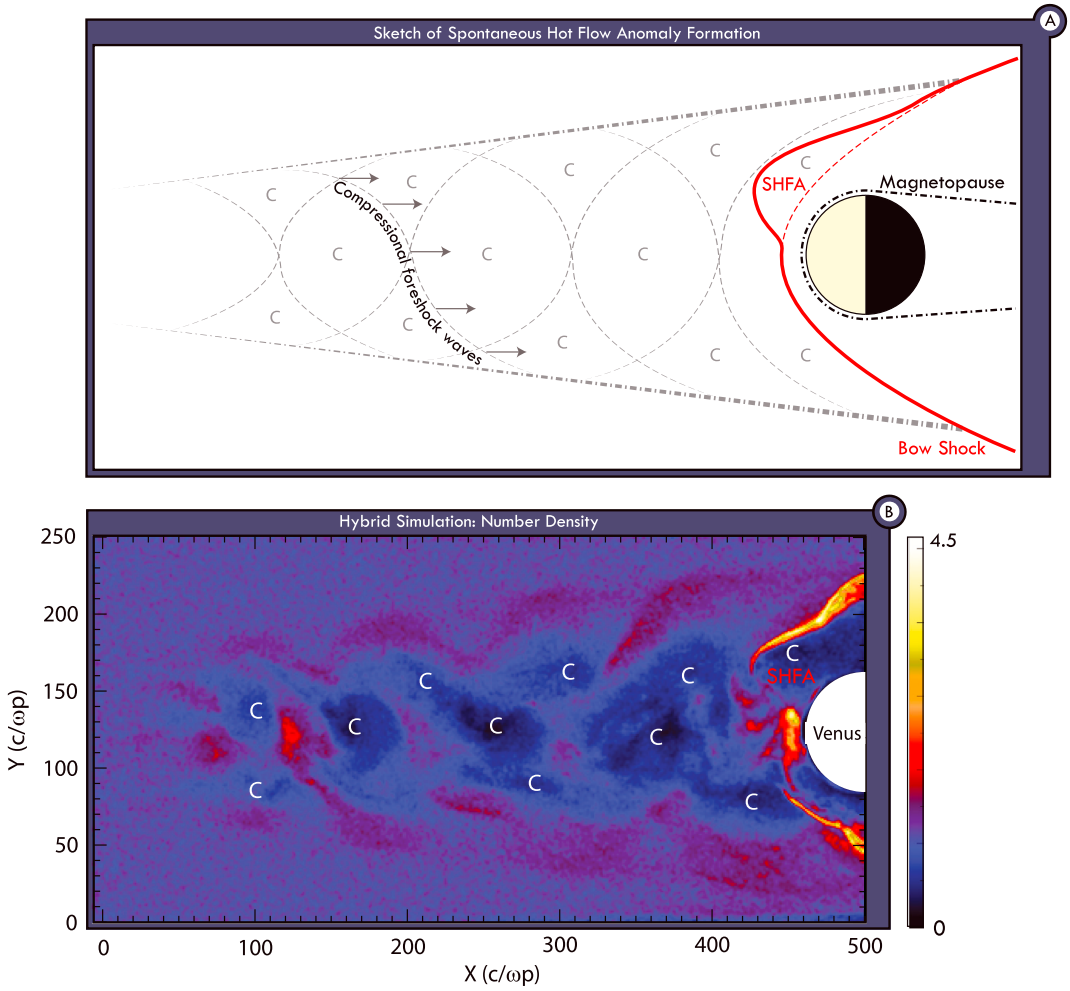

Figure 1. (a) Sketch of the foreshock of an unmagnetized planet (e.g., Mars and Venus) under radial IMF conditions (oriented parallel to the Sun-Planet line, *x* axis). The bow shock is shown in red, with an attached SHFA. The foreshock is shown in grey, a field of cresting compressional foreshock waves and troughs, forming "foreshock cavitons" (marked with a "C"). (b) Hybrid simulation of the foreshock of an unmagnetized planet showing the same view denoted in Figure 1a. The color denotes relative particle density with respect to the solar wind. Cavitons are again denoted with a C.

shock [*Tsurutani and Rodriguez*, 1981; *Hoppe and Russell*, 1983] or produced locally [*Hellinger and Mangeney*, 1999; *Mazelle et al.*, 2003; *Meziane et al.*, 2004]. The waves attempt to propagate upstream but are convected back toward the bow shock by the solar wind. As they convect deeper into the foreshock, they enter regions of higher ion density. These ions alter the index of refraction for the medium causing transverse modes to become compressive, and thus the waves can steepen [e.g., *Collinson et al.*, 2012b; *Wilson et al.*, 2009; *Tsubouchi and Lembège*, 2004; *Tsurutani et al.*, 1987, and references therein]. They become more oblique and compressional the deeper they go.

One of the possible resulting foreshock phenomena is a "*caviton*" [*Blanco-Cano et al.*, 2011]. Cavitons are localized troughs in density and magnetic magnitude resulting from the field of compressive ULF foreshock waves [*Blanco-Cano et al.*, 2009; *Kajdič et al.*, 2011, 2013]. They form continuously and regularly in the foreshock and are swept back toward the bow shock along by the advection of the solar wind. Hybrid simulations by *Omidi et al.* [2013] of Earth's foreshock show that occasionally as a caviton approaches the bow shock, it undergoes a rapid transformation into an SHFA as a result of interactions with the bow shock. The plasma within becomes heated and even more diffuse, resulting in a signature identical to that of HFAs, but without the need for any IMF discontinuity. The specific heating mechanism remains unknown but may result from ion trapping by the cavitons and ion reflection between the bow shock and the cavitons [*Omidi et al.*, 2013].

2.3. Hybrid Simulation of SHFA Formation at Venus

In order to investigate the structure of the Cytherean foreshock, *Omidi et al.* [2017] have conducted 3-D global hybrid (kinetic ions, fluid electrons) simulations of solar wind interaction with Venus. Figure 1b shows the proton density from a run with radial IMF which illustrates the ion foreshock and the dayside bow shock and magnetosheath. The results show that the interaction between the solar wind and the backstreaming ions in the foreshock results in the excitation of parallel (to the magnetic field) and oblique ULF waves (on the fast magnetosonic branch) whose nonlinear evolution result in the formation of the cavitons seen in Figure 1b. The excited ULF waves and cavitons are carried toward the bow shock by the solar wind resulting in the formation of SHFAs at the shock. The results observed here are similar to those seen in hybrid simulations of the Earth's bow shock with the size of the cavitons and SHFAs at the two planets being comparable (~0.5 to 1 Earth Radii). However, given the much smaller size of the Cytherean bow shock and magnetosheath, even a single SHFA has a global impact on the system. Full details of our global hybrid simulations can be found in the companion paper *Omidi et al.* [2017], and this brief description is included in this observational study purely to establish that this phenomenon has been recently predicted to occur at unmagnetized planets.

3. A Spontaneous Hot Flow Anomaly at Mars

Figure 2 shows a map of orbit № 2472 (7 January 2016) of the *MAVEN* Mars Scout (red), with a typical modeled bow shock and magnetic pileup boundary according to *Vignes et al.* [2000] (black). At 01:33 Greenwich Mean Time (GMT) (gold star), *MAVEN* was on the flanks of the magnetosphere, slightly upstream of the bow shock, when it encountered two events exhibiting all expected plasma properties of SHFAs or classic HFAs. However, no associated magnetic discontinuity in the IMF was observed, consistent with these events being SHFAs.

Figure 3 shows multi-instrument observations from *MAVEN* on two time scales. Figures 3a–3d cover the 3 min period from 01:32:30 to 01:35:30 GMT so that the field and particle perturbations can be more easily contrasted against background foreshock conditions. Figures 3e–3h show a 1 min close-up of the primary candidate SHFA from 01:33:00 to 01:34:00 GMT. Figure 3 is organized thus: Panels a and e show a color-coded timeline of the event. Periods when the *MAVEN* was in the foreshock are blue, the core of the SHFA in gold, and the bounding compression regions in purple. Figures 3b and 3f show magnetometer data in MSO coordinates. Each component is plotted separately with θ_n, the angle that the magnetic field vector makes with the normal to the *Vignes et al.* [2000] Martian bow shock of Mars, plotted beneath. Finally, Figures 3c and 3g show ion observations from the Solar Wind Ion Analyzer, with time/energy spectrogram on top, and ion density, temperature, and velocity plotted beneath. Finally, Figures 3d and 3h show electron observations from solar wind electron analyzer, with spectrogram on top, and corresponding density and temperature plotted beneath.

We shall now describe these observations in two levels of detail: Firstly, a brief summary overview, and then a more detailed description of the observations of each instrument.

3.1. Overview of *MAVEN* Observations

MAVEN encountered two candidate SHFA events within minutes of each other. Both have magnetic signatures consisted with the SHFAs reported at Earth by *Zhang et al.* [2013]: spiked $|B|$ in the compression regions (i.e., the peaks), reduced $|B|$ in the core (with respect to the background IMF), and neither event being associated with an IMF discontinuity. Whilst hotter and less dense plasmas (both ions and electrons) were observed in the core regions of both events (consistent with SHFAs), they are more pronounced in the first event. Similarly, whilst the expected increase in ion and electron densities were observed in both bounding compression regions of the first event, they are not as well resolved in the second. Therefore, whilst the collected magnetic and plasma observations for both events are consistent with SHFAs, the first event currently represents our best, primary candidate. We shall now describe the measurements made by each of these three instruments in detail.

3.2. *MAVEN* Magnetometer

Figures 3b and 3f show *MAVEN* magnetometer observations at 32 samples per second. Plotted are the magnitude ($|B|$), the three components vector (Bx, By, Bz), and the angle that the magnetic field makes with the bow shock of Mars (θ_n). Both the primary event at 01:33 GMT and the secondary event at ~01:35 exhibit all the magnetic signatures of an SHFA: Firstly, both events were observed in the foreshock, the region where SHFAs are known to form. Secondly, in the core of the events, there is a strong drop in ($|B|$) below ambient IMF values.

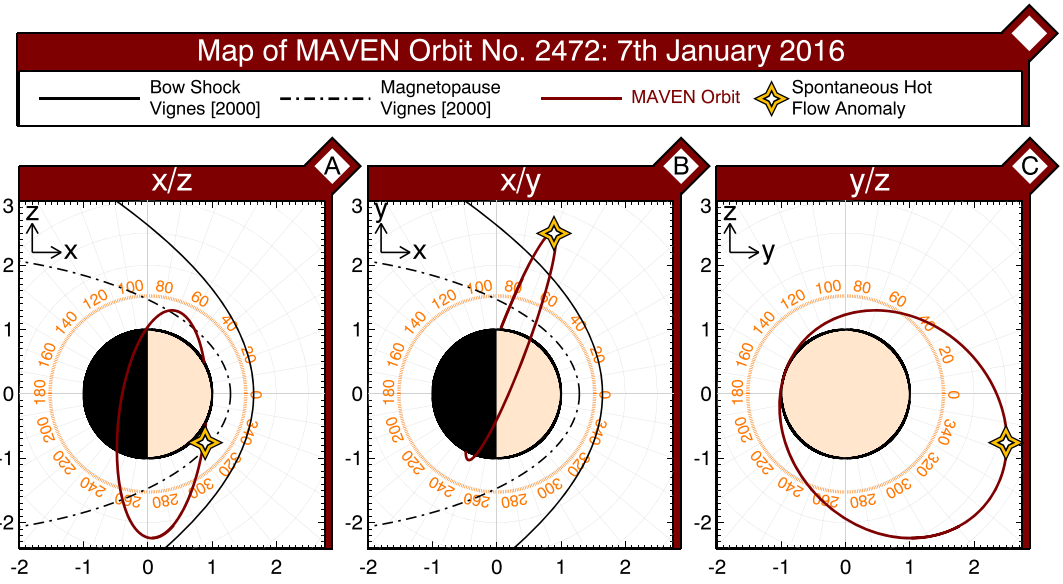

Figure 2. Map of *MAVEN* orbit № 2472 in Mars Solar Orbital (MSO) coordinates showing the location of the SHFA in Figure 3.

Thirdly, there are bounding $|B|$ enhancements associated with the bounding compressive regions. These magnetic signatures are in most ways very similar to the classic Martian HFA reported recently by *Collinson et al.* [2015], with one important distinction. Consistent with these events being SHFAs, no attendant IMF discontinuity was observed, and the ambient magnetic field remained in the same average orientation after the event as before it. Thus, we conclude that these HFA-like foreshock transients formed spontaneously in the Martian foreshock without an interplanetary current sheet or discontinuity.

One potential inconsistency with this event being an SHFA is its being observed in the quasi-perpendicular foreshock ($\theta_n \approx 90°$), whereas our simulations and current theory predict that SHFAs form in the quasi-parallel foreshock ($135° > \theta_n < 45°$). However, given that foreshock transients convect with the solar wind, it is possible that this event formed elsewhere (upstream of the spacecraft in the parallel region of the foreshock) and was then blown over *MAVEN*. Thus, the fact that this SHFA candidate was observed in the quasi-perpendicular foreshock is not an absolute barrier to it being an SHFA, it simply means that it is unlikely to have formed at this location and may represent a more well-developed example. This hypothesis is strengthened by the fact that this would not be the first foreshock transient to have been observed at a distance from where it formed: such an evolutionary story (distant formation and then being blown over the spacecraft a few minutes afterward) would be identical to the classical Martian HFA reported by *Collinson et al.* [2015], which had formed on the other side of the bow shock and had been advected over the whole Martian magnetosphere.

3.3. *MAVEN* Solar Wind Ion Analyzer (SWIA)

Figures 3c and 3g show data from the *MAVEN* Solar Wind Ion Analyzer (SWIA) [*Halekas et al.*, 2013]. SWIA has a 360° × 90° field of view and makes a full 3-D ion distribution once every 4 s. An ion spectrogram is shown for both time intervals, with time on the *x* axis and energy on the *y* axis with the color denoting the $\log_{10}$ of the counts per bin. The solar wind can be seen as a bright continuous red/orange line at ≈2 keV. Beneath the spectrograms are plotted density, temperature, and velocity moments, calculated at 4 s resolution. Consistent with SHFAs, the core of both events was characterized by a decrease in particle density and an increase in ion temperature. However, the ion perturbations are far more pronounced in the primary example (Figure 3g), with a 2 order of magnitude decrease in density. Whilst ion flow perturbations were observed, they were very modest when compared to SHFAs at Earth [*Zhang et al.*, 2013]. This is consistent with the relatively anemic ion flow perturbation exhibited by the "classical" Martian HFA reported by *Collinson et al.* [2015]. The event was so brief that SWIA was unable to return 3-D ion distributions to sufficiently resolve two-component proton from alpha moments for this event. Thus, the temperature shown in Figure 3 is calculated from the Ty and Tz components which were not subject to alpha contamination and was calculated using $T_{\text{effective}} = \left(T_y + T_z\right)/2$.

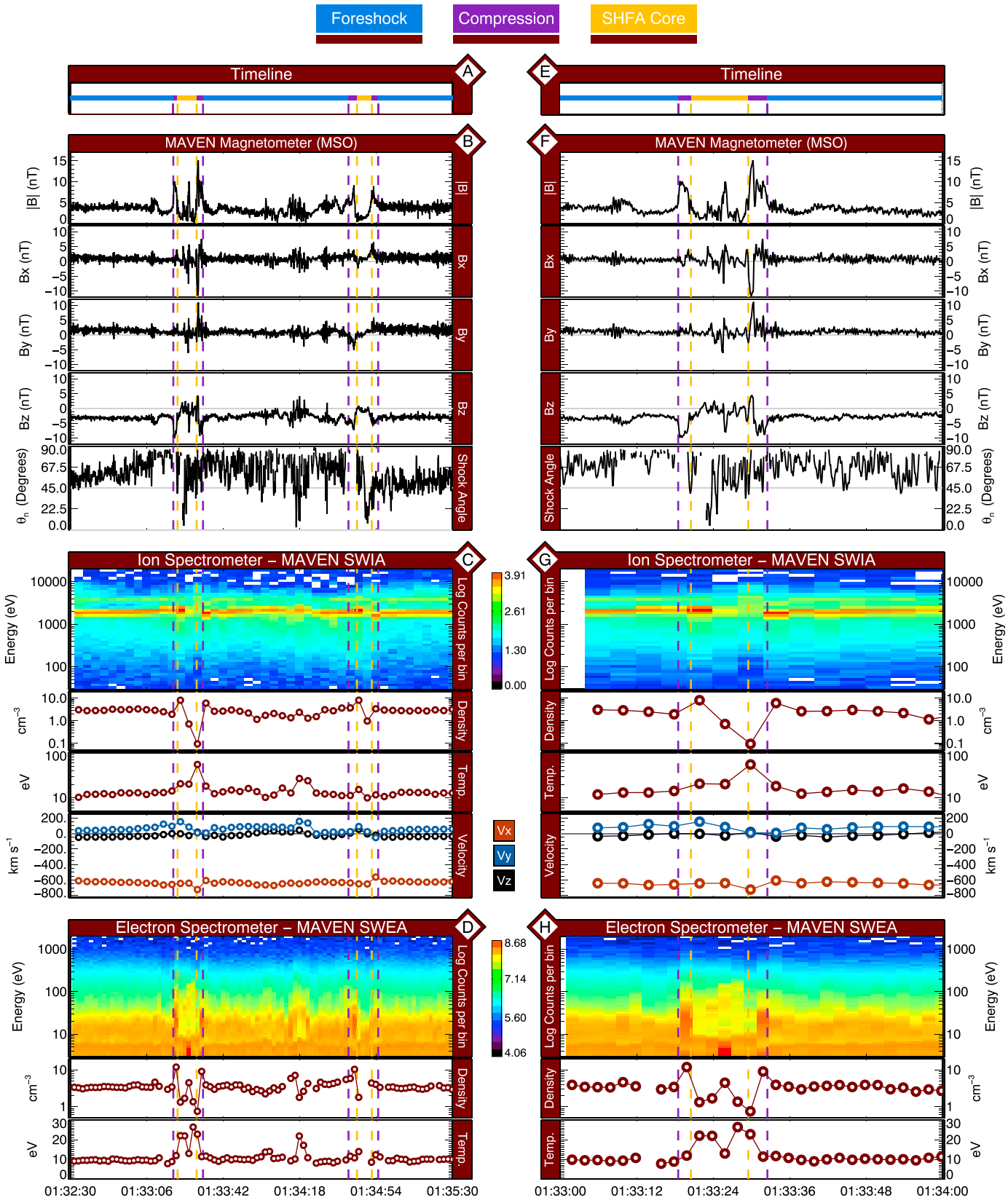

Figure 3. An SHFA observed in the Martian foreshock by *MAVEN* on 7 January 2016. (e–h) One minute of data to present a close-up of the event. (a–d) A longer (3 min) interval of data so that the SHFA can be compared against background solar wind conditions and a possible second event occurring shortly thereafter.

Table 1. MAVEN SWIA Solar Wind Plasma Moments Before and During the Core of the Martian SHFA

Region	Time Interval (GMT)	Density (cm^{-3})	Velocity (km/s) Vx	Vy	Vz	|V|	Temp. (eV)	$P_{dynamic}$ (pPa)
Foreshock	01:33:04 to 01:33:16	2.64	−652	92	−21	659	49	960
SHFA core	01:33:24	0.73	−641	84	−27	647	45	256
	01:33:28	0.10	−723	9	17	723	304	8

Whilst the first event (the primary candidate shown in Figure 3g) exhibited all the canonical ion signatures of an SHFA, the evidence from Solar Wind Electron Analyzer (SWEA) for the secondary candidate (occurring later at ~01:35) is less clear cut. Although a modest increase in ion density is observed with the first compression region, none is observed for the second compression region, and the changes in ion density and temperature in the core are even more moderate. However, given the shorter duration of the second event, and its compelling SHFA-like magnetic signature, it is still quite plausible that this event was an SHFA.

Table 1 shows average solar wind plasma moments from before the primary event, and the two measurements made inside the core region of the SHFA. As with the *Collinson et al.* [2015] "classic" Martian HFA, although the velocity perturbations were mild, the density decreased by an order of magnitude, driving a 2 order of magnitude decrease in the solar wind dynamic pressure. We shall later discuss the potential impact of this on the ionosphere and induced magnetosphere of Mars.

3.4. *MAVEN* Solar Wind Electron Analyzer (SWEA)

Figures 3d and 3h show electron spectrograms, plus initial estimates of density and temperature measured by the Solar Wind Electron Analyzer (SWEA) [*Mitchell et al.*, 2016]. SWEA has a 360° × 120° field of view and during this period was operating in "solar wind" mode (see Table 4 of *Mitchell et al.* [2016] for a summary of SWEA operational modes), whereby it returned plasma moments every 4 s. As with *Collinson et al.* [2015], these moments are preliminary until the spacecraft potential from the *MAVEN* Langmuir Probe and Waves (LPW) experiment can be utilized to remove spacecraft electrons. Consistent with an SHFA, in the compression regions of the primary SHFA candidate, SWEA observed increases in electron density comparable to that observed by SWIA and a modest increase in electron temperature. In the core, electron temperature tripled from 10 eV to 30 eV, and the density decreased by an order of magnitude. The decrease in density is not as pronounced as in SWIA ion observations because of the contribution to the density of the aforementioned spacecraft photoelectrons.

4. A Spontaneous Hot Flow Anomaly at Venus

Almost 4 years previously, and approximately 0.9 AU closer to the Sun, at approximately 02:26 GMT on 18 October 2012, the ESA *Venus Express* spacecraft was just upstream of the Venusian bow shock when it was engulfed by an explosive foreshock transient with almost identical properties to those observed by *MAVEN* at Mars, exhibiting all the properties expected of an SHFA. Figure 4 shows a map of orbit № 2372. The trajectory of the *Venus Express* is shown in blue, and the location of the SHFA candidate is denoted by a gold star. Figure 5 shows ion and electron observations by the *Venus Express* "Analyzer of Space Plasmas and EneRgetic Atoms" (ASPERA) [*Barabash et al.*, 2007] and Magnetometer (MAG) [*Zhang et al.*, 2006]. Figures 5a–5d show a 10 min interval so that the perturbations associated with the SHFA candidate may be better compared with background solar wind conditions, and Figures 5e–5h show a close-up of currently our best candidate for a Venusian SHFA.

As with the Martian SHFA candidate, we shall again first give a brief overview and then a more detailed description of these observations.

4.1. Overview of *Venus Express* Observations

The magnetometer aboard *Venus Express* is comparable in performance to that aboard *MAVEN*, and thus the magnetic signature of the Venusian SHFA candidate is well resolved and very similar to the Martian candidates shown in Figure 3, and again is comparable to SHFAs observed at Earth [*Zhang et al.*, 2013]. The associated plasma perturbations are not as resolved due to the limited temporal resolution of the ASPERA Ion Mass Analyzer (IMA) and several orders of magnitude lower sensitivity of the electron spectrometer [*Collinson et al.*, 2009]. However, consistent with past observations of classic HFAs at Venus and what would be expected for

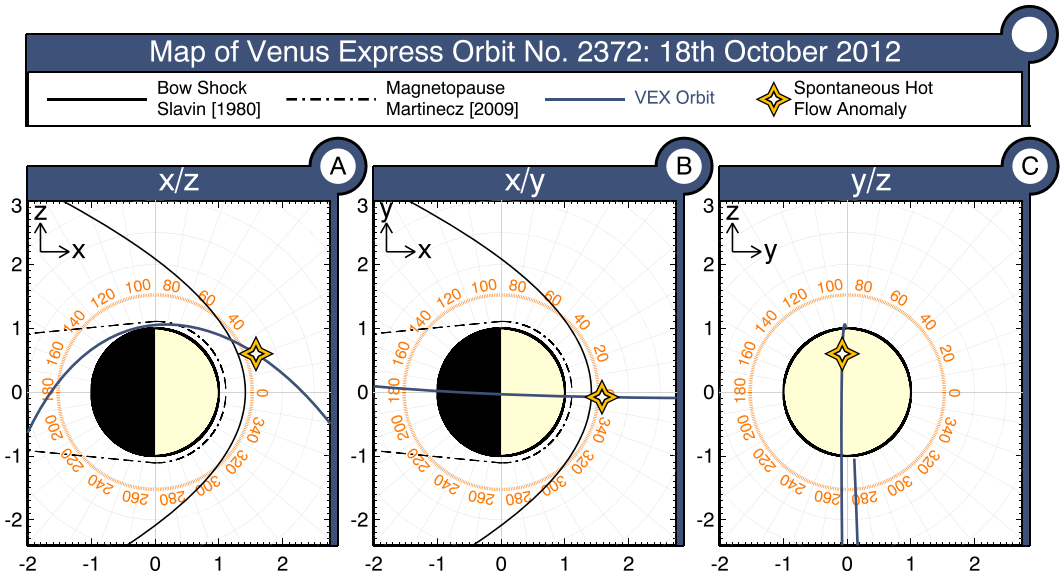

Figure 4. Map of *Venus Express* orbit № 2372 in Venus Solar Orbital (VSO) coordinates showing the location of the SHFA in Figure 5.

an SHFA: (1) IMA observes evidence for a protonic disturbance with ions coming from unexpected directions, consistent with a flow deflection or heating, although the strongest disturbances occurred just prior to the magnetic and electron signatures; and (2) Electron Spectrometer (ELS) observes a decrease in electron density in the core of the event and density enhancements in the bounding compression regions. We shall now describe these observations in detail.

4.2. *Venus Express* Magnetometer

Figures 5b and 5f show observations made at 32 Hz resolution by the *Venus Express* Magnetometer (MAG). The event itself took only ~30 s to pass the spacecraft and left a magnetic signature with all the main features of a Hot Flow Anomaly. However, as with the Martian event, the IMF has the same orientation before and after, there is no evidence for the presence of a solar wind tangential discontinuity required for the formation of a classic HFA, and thus this event is consistent with an SHFA.

Within the core of the event, the total magnetic field strength ($|B|$) drops with respect to the background IMF, which is exactly what would be expected for an SHFA. This core is bounded by two regions where the magnetic field is slightly stronger than in the surrounding solar wind, which as with the events at Mars, we attribute to weakly shocked plasma that is being compressed as the SHFA rapidly expands into the surrounding solar wind. Of the two compressional regions, the later has a stronger spike in $|B|$. Given that SHFAs convect with the solar wind, this stronger compressional spike is on the upstream side of the event. As with previous observations of classic HFAs at Venus by *Collinson et al.* [2012a], this is as one would expect with an SHFA with a stronger compression on the side that is expanding against the flow of the supersonic solar wind.

The lower panels of Figures 5b and 5f show plots of the angle that the magnetic field vector makes with the bow shock of Venus (θ_n). Consistent with an SHFA, the event was in the quasi-parallel foreshock, and there is no significant change after the event which might indicate the presence of an IMF discontinuity.

4.3. *Venus Express* ASPERA Ion Mass Analyzer (IMA)

Figures 5c and 5g show data from the ASPERA Ion Mass Analyzer (IMA). ASPERA-IMA scanned through a 360° ± 45° field of view in 192 seconds using 16 steps of its electrostatic deflector plates. Thus, unlike the continuous *MAVEN* SWIA spectrograms shown in Figures 3c and 3g (each time interval representing a full 2π distribution), the ASPERA-IMA spectrograms in Figures 5c and 5g show the counts at each deflector plate setting, with the deflection (elevation) angle plotted below.

The period covered by Figure 5c was sufficient for approximately three scans of the sky by IMA. Four ion populations were observed. Three of the populations occurred regularly in every deflector plate scan and are

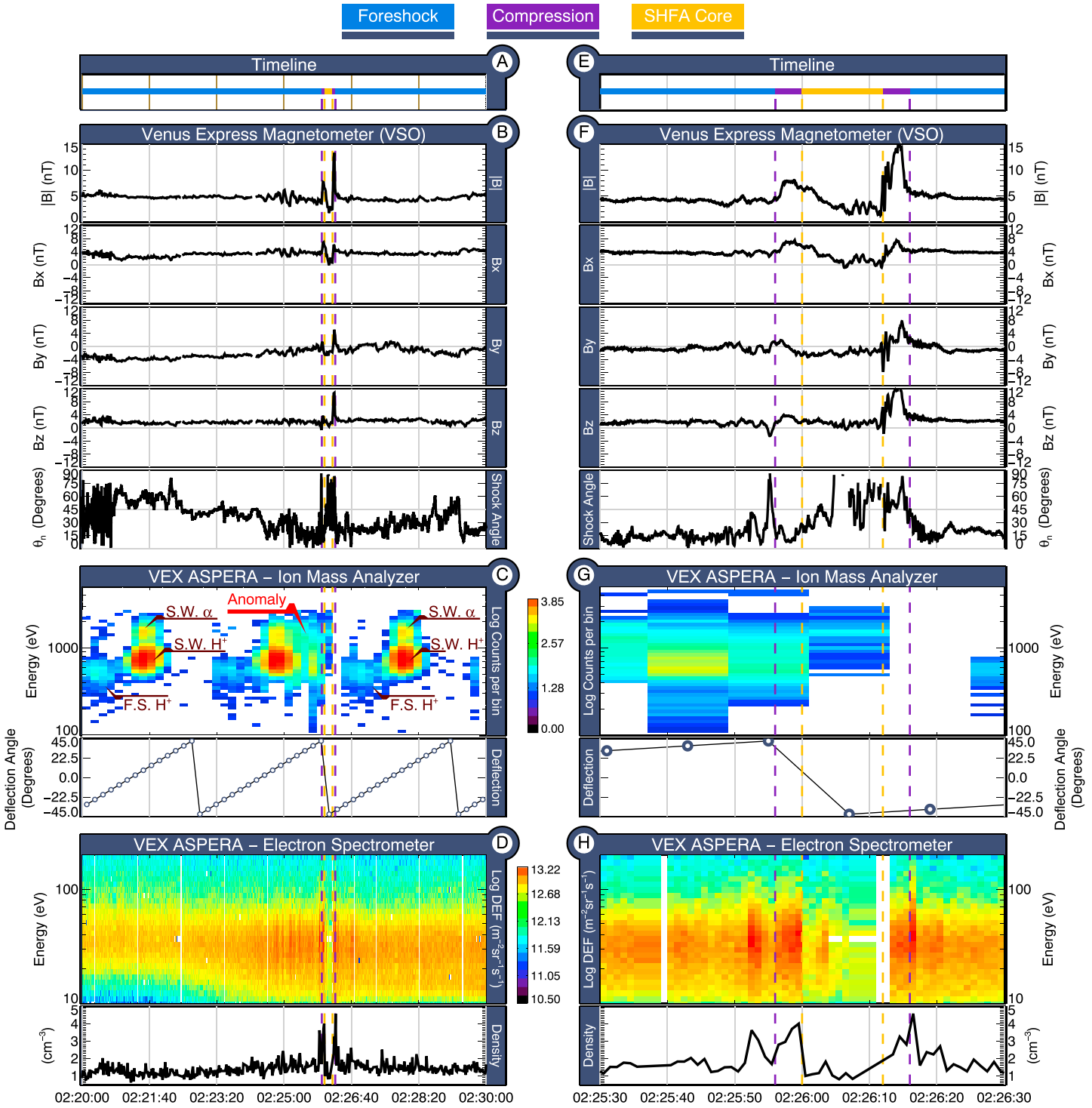

Figure 5. An SHFA encountered in the Venusian foreshock on 18 October 2012 by the ESA *Venus Express* whilst just upstream of the bow shock. (e–h) A 1 min interval of data to provide a close-up of the event (from 02:25:30 to 02:26:30 Greenwich Mean Time). (a–d) A longer 10 min interval of data (from 02:20:00 to 02:30:00 Greenwich Mean Time) so that the event can be compared against the background conditions in the solar wind.

labeled in maroon in Figure 5c. These three populations are (1) an anti-sunward beam of solar wind protons (S.W. H^+), (2) a more energetic anti-sunward beam of solar wind alpha particles (S.W. α), and (3) a foreshock population of solar wind protons (F.S. H^+) backscattered by the Venusian bow shock.

In addition to these regular, repeating ion populations, an additional anomalous proton population was observed just prior to and during the SHFA candidate (labeled "anomaly" in red in Figure 5c). As with the previous studies of classic HFAs at Venus such as *Collinson et al.* [2012a, 2014], the 192 s cadence of IMA means that we cannot resolve these protonic perturbations. However, as with *Collinson et al.* [2012a, 2014], the fact that energetic ($\sim$ 1 keV) protons are observed coming from an unexpected direction is consistent with an ion flow or temperature anomaly, as one would expect with an SHFA. It is very interesting to note that unlike "classic" HFAs at Venus, much of the anomalous population of protons were observed just prior to the SHFA and were observed coming from the direction of the planet (i.e., the bow shock). Since our simulations show that as at Earth, SHFAs form through interaction between foreshock cavitons and the bow shock, we speculate that these anomalous protons prior to the event may be a result of solar wind protons bouncing back and forth between the bow shock and a foreshock caviton, resulting in its transformation into an SHFA that was then blown over the *Venus Express* by the solar wind. Such an interpretation would be consistent with one of the formation mechanisms of terrestrial SHFAs suggested by *Omidi et al.* [2013]. However, since IMA cannot resolve the perturbed ion perturbations, all that can be said with certainty is that consistent with an SHFA, the local ion environment was perturbed.

4.4. *Venus Express* ASPERA Electron Spectrometer (ELS)

Figures 5d and 5h show data from the ASPERA-4 Electron Spectrometer (ELS). On top are time-energy spectrogram where the color of the plot denotes the $\log_{10}$ of the electron differential energy flux (m^{-2} sr^{-1} s^{-1}), with electron density labeled below.

ASPERA-ELS suffers from two major limitations when compared to MAVEN-SWEA. Firstly, ASPERA-ELS had a very limited 2-D field of view (as opposed to the 2π f.o.v. of MAVEN-SWEA), and thus this density should be considered a "pseudo" plasma moment calculated assuming isotropy. Thus, while it may be examined for evidence of qualitative changes in relative density, in this instance it should not be relied upon as an absolute *quantitate* measurement of the absolute number density at Venus. The second limitation of ASPERA-ELS is that its sensitivity is an order of magnitude lower than designed due to manufacturing defects [*Collinson et al.*, 2009], and several orders of magnitude lower than MAVEN-SWEA, and thus during brief transient low density environments such as the core of an SHFA or HFA, there are typically insufficient counting statistics to generate higher-order moments such as temperature.

However, whilst ASPERA-ELS is more limited in its capabilities than MAVEN-SWEA, all of its observations during the event are consistent with what would be expected during an SHFA. They are also identical (in both nature and quality) to those which established the presence of classic HFAs at Venus [*Collinson et al.*, 2012a]. In the core of the SHFA candidate, where the magnetic field strength is very low ($|\mathbf{B}| \approx 0$), there is a clear decrease in electron flux, indicative of a sudden drop in electron density, velocity, or both. This is consistent with observations within the core regions of SHFAs at Earth where the velocity of the plasma has been observed to drop dramatically, and density falls below solar wind values. In this instance, the pseudo-density calculated assuming isotropy suggests that this reduction in flux is at least in part due to decrease in density, consistent with the core of an SHFA.

In the compression regions where the magnetic field peaks, ELS records a jump in electron flux over a wide range of energies, and the pseudo-density suggests a fivefold increase in the density of solar wind electrons. This is consistent with our interpretation of this region as a region of dense plasma strongly compressed by the rapid expansion of the SHFA. Curiously, in addition to the spikes in electron density associated with magnetic field enhancements, another electron flux and density enhancement is observed just prior to the first (downstream) compression region.

5. Discussion

In this paper we presented two case studies of candidate Spontaneous Hot Flow Anomalies (SHFA), one at Mars and the other at Venus. Both exhibited similar magnetic and plasma properties to those observed at Earth, although the solar wind velocity perturbations observed by *MAVEN* at Mars were very much weaker than those reported at Earth by *Zhang et al.* [2013]. Since similarly weak flow perturbations were reported in

Table 2. Calculation of Solar Wind Proton Gyroradius for Each Event

	Velocity (km/s)				IMF (nT)					$V_{\|\|}$	$V_{\perp}$	H^+ gyroradius	SHFA Size
Planet	*Vx*	*Vy*	*Vz*	$\|V\|$	*Bx*	*By*	*Bz*	$\|B\|$	$\|\hat{B}\|.\|\hat{V}_{SW}\|$	(km/s)		(km)	(km)
Mars	−623	13	−61	627	−3.13	1.83	−0.90	3.74	0.85	531	333	≈ 928	≈ 7300
Venus	−302	−58	−159	347	3.79	3.79	−1.07	2.24	4.67	318	138	≈ 308	≈ 5900

a classical HFA at Mars [*Collinson et al.*, 2015], one important topic for future statistical studies of foreshock transients at Mars is whether this is typical, and if so would be a key difference between those observed at Earth's much larger foreshock.

Despite occurring at different planets, the Martian and Venusian SHFAs are very similar in many key respects. Firstly, their durations: Measuring from the peak in $|B|$ in the first compression region to the peak in $|B|$ second compression region, the Martian SHFA lasted approximately 11 s (01:33:19 to 01:33:30 GMT), whereas the Venusian SHFA lasted ≈17 s (02:25:57 to 02:26:14 GMT). With only a single spacecraft it is not possible to measure the expansion rate of these events; however, assuming that they are quasi-static (unlikely to be the case, but the best that can be done), we may attain a very rough first-order estimate of their scale by also assuming that they are convecting at exactly the solar wind speed (V_{SW}). As shown in Table 2, this approach suggests that the Martian SHFA was approximately 7300 km across. At Venus, while the 192 s temporal resolution of ASPERA-IMA is insufficient to resolve the ionic perturbations associated with the SHFA, it is more than capable of measuring the bulk solar wind velocity in which the SHFA is embedded, and we estimate a size of approximately 5900 km. These dimensions may be anecdotally compared to the ≈13, 000 km SHFA reported at Earth by *Zhang et al.* [2013] (30 s duration, propagation speed of 420 km/s). While not a statistical comparison, it is known that "classical" HFAs scale with the size of the magnetosphere [*Collinson et al.*, 2014, 2015], and thus it is plausible that SHFAs may be generally smaller at Mars and Venus than at Earth due to the smaller size of solar wind obstacle.

Next we estimated how large these events were with respect to the local proton gyroradius, r_g, according to equation (1).

$$r_g = \frac{mv_{\perp}}{|q||B|} \tag{1}$$

where m and q are the mass and charge of a proton, and $v_{\perp}$ is the component of the solar wind velocity perpendicular to the magnetic field B. In order to determine $v_{\perp}$, we first determined the component of the solar wind velocity parallel to the magnetic field ($v_{||}$) by multiplying the magnitude of the solar wind velocity ($|V_{SW}|$) with the dot product of unit vectors of velocity ($|\hat{V}_{SW}|$) and magnetic field ($|\hat{B}|$), as in equation (2).

$$v_{||} = |V_{SW}|(|\hat{B}|.|\hat{V}_{SW}|) \tag{2}$$

The perpendicular component of the solar wind $V_{\perp}$ may then be determined simply via $V_{\perp} = \sqrt{V_{SW}^2 - V_{||}^2}$, which may be put back into equation (1) to calculate the *convected* proton gyroradius. Note that this is distinctly different (and much larger) from the thermal proton gyroradius. When the resulting convected proton gyroradii were calculated, the Martian SHFA was found to be approximately 7.9 times larger than the local proton gyroradius (≈928 km), whereas the Venusian SHFA was approximately 19.1 times larger than the local proton gyroradius (≈308 km). Thus, the Martian SHFA was larger in a physical sense, but smaller than the Venusian example in terms of the natural "yard stick" of proton gyroradius. This may be a result of the Venusian example forming at a larger solar wind obstacle, or possibly being a more well-developed example.

As with "classic" Hot Flow Anomalies at Mars and Venus, these events are very large when compared to the size of the system. The Martian SHFA was approximately 2.3 Martian Radii across (R_M = 3390 km), and the Venusian SHFA was approximately 1 Venus Radii across (R_V = 6052 km), consistent with our recent hybrid simulations [*Omidi et al.*, 2016]. Unlike at Earth where the interaction between SHFAs and the planet is mediated by the magnetosphere, these unmagnetized planets have no such magnetic shield, and as with classic HFAs, these events have the potential to impart energy directly into the ionosphere. The SHFA forms a bubble on the outside of the bow shock of the planet, deflecting solar wind flow and creating a vacuum which the ionopause may expand upward into. Following *Collinson et al.* [2015], for a first-order approximation as to how far the location of the Martian ionopause (R_i) might shift from its nominal radial distance (R_r) as a response

to the observed pressure pulse at Mars, we assume a simple static Newtonian pressure balance as below in equation (3).

$$(R_i - R_r) = -H \ln\left(\frac{P_i}{P_r}\right) \quad (3)$$

If we assume that, as with *Collinson et al.* [2015] Martian HFA, the change in pressure is dominated by the dynamic pressure of the solar wind, then this highly simplistic model suggests this SHFA increased the scale height of Martian topside ionosphere ($H \approx 40$ km [*Withers*, 2009]) by ~200 km. Work is currently underway to implement an ionosphere into our hybrid models which will enable a better insight into the effects of foreshock transients on the ionospheres of unmagnetized planets.

At Earth, SHFAs are an inherent part of shock dissipation process with significant impacts on the magnetosheath and magnetopause [*Omidi et al.*, 2014, 2016; *Gutynska et al.*, 2015]. *Omidi et al.* [2017] found that at Venus the pressure variations associated with cavities and SHFAs in the Venusian magnetosheath result in a continuous sunward and anti-sunward magnetopause motion. This result is consistent with previous suggestions that SHFAs may be responsible for the generation of ion cyclotron waves and precipitation of ring current protons in the outer magnetosphere. For full details of our hybrid models and their results, see the companion paper, *Omidi et al.* [2017].

6. Summary

In this paper we presented case studies of explosive compressional foreshock transients at Mars and Venus, in both cases exhibiting magnetic and plasma perturbations entirely consistent with our current understandings of SHFAs observed at Earth, and as predicted by our hybrid simulation:

1. At both planets, comparable magnetic signatures were observed consistent with SHFAs; low $|B|$ in the core of the event; spiked $|B|$ in the bounding compressional regions; and no change in the direction of the interplanetary magnetic field after the event (i.e., no IMF tangential discontinuity as for a classic HFA).
2. At both planets, electron density depletions were observed in the core, and electron density enhancements in the bounding shock-like compressional regions resulting from the SHFA's explosive expansion against the solar wind.
3. At Mars, enhancements in ion and electron temperature could be observed, together with a mild perturbation in the solar wind velocity. At Venus, whilst these signatures are also expected, and are possibly suggested by perturbations observed in ion and electron spectrograms, they cannot be resolved due to instrumental limitations.

Thus, at Mars, *MAVEN* recorded a comprehensive set of all the expected magnetic, electron, and ion perturbations, and we therefore conclude it to be the Martian equivalent of a Spontaneous Hot Flow Anomaly. Mere minutes later, a second candidate event was encountered by *MAVEN*. Whilst the plasma perturbations in this second event are not as clear cut and canonical as in our primary candidate, nonetheless the overall nature of the event (as shown in both its magnetic signature and SWIA/SWEA spectrograms) is quite consistent with that of the primary candidate, and thus we conclude that it is highly plausible that this secondary event was also an SHFA.

Whilst at Venus the set of observations is less complete than at Mars due to instrumentational limitations, all are consistent with the presence of an SHFA. Thus, although we cannot fully resolve all the associated plasma perturbations as well as with *MAVEN* due to the paucity of data, when combined with a compelling well-resolved SHFA-like magnetic signature and the fact that SHFAs are predicted at Venus by our hybrid simulations (Figure 1), we conclude that the most plausible explanation for these collected observations is that *Venus Express* encountered a Spontaneous Hot Flow Anomaly.

To summarize, all three of these events are practically identical to the "classic" HFAs previously reported at Mars [*Øieroset et al.*, 2001; *Collinson et al.*, 2015] and Venus [*Slavin et al.*, 2009; *Collinson et al.*, 2012a, 2014], but with the crucial distinction that there is no evidence for the presence of an IMF discontinuity. Given that the distinction between HFA and SHFA is entirely due to the presence or absence of such an associated IMF discontinuity, by definition, these HFA-like events must be classified as SHFAs. This conclusion is further supported by our hybrid simulations [*Omidi et al.*, 2017] which predict that SHFAs can form in the foreshocks of unmagnetized planets through the same mechanism as at Earth (i.e., the interaction of foreshock cavitons with the

bow shock), and our observations at Mars and Venus are consistent with that predicted by this simulation. Through first-order estimation of the size of the events with respect to the local proton gyroradius, we find that the Venusian SHFA was effectively larger than the Martian event (≈19 gyroradii versus ≈7). This may be a result of forming at a larger solar wind obstacle or may represent a more well developed example of an SHFA.

We thus conclude that Spontaneous Hot Flow Anomalies form even in the relatively small foreshocks of the unmagnetized planets of Venus and Mars, and their presence at these tiny magnetospheres is suggestive that they may be a fundamental and universal phenomena, occurring upstream of any planetary or celestial bow shock. Our simulations show that they form in a similar manner as at Earth, through the rapid evolution of a foreshock caviton into an SHFA. The establishment of the presence of SHFAs at Mars and Venus raises several scientific questions for future investigations: How common are they? Do they form under all IMF angles and conditions? What is the impact on the planet? Spontaneous Hot Flow Anomalies are known to drive global magnetospheric perturbations at Earth, and we postulate that as with "classical" HFAs, they have the potential to directly impact the topside ionospheres at Mars and Venus, a topic which we intend to pursue in the future.

Acknowledgments
MAVEN data are available from the NASA Planetary Data System, and *Venus Express* data from the ESA Planetary Science Archive. This work was supported by NASA Solar System Workings Program grant NNX15A176G. The ASPERA-4 team are grateful to NASA for allowing the ELS flight spare (constructed under contract NASW-00003) to be flown on the *Venus Express* as part of ASPERA-4.

References

Asbridge, J. R., S. J. Bame, and I. B. Strong (1968), Outward flow of protons from the Earth's bow shock, *J. Geophys. Res.*, *73*, 5777–5782, doi:10.1029/JA073i017p05777.

Barabash, S., et al. (2007), The Analyser of Space Plasmas and Energetic Atoms (ASPERA-4) for the Venus Express mission, *Planet. Space. Sci.*, *55*, 1772–1792.

Blanco-Cano, X., N. Omidi, and C. T. Russell (2009), Global hybrid simulations: Foreshock waves and cavitons under radial interplanetary magnetic field geometry, *J. Geophys. Res.*, *114*, A01216, doi:10.1029/2008JA013406.

Blanco-Cano, X., P. Kajdič, N. Omidi, and C. T. Russell (2011), Foreshock cavitons for different interplanetary magnetic field geometries: Simulations and observations, *J. Geophys. Res.*, *116*, A09101, doi:10.1029/2010JA016413.

Collinson, G., et al. (2015), A hot flow anomaly at Mars, *Geophys. Res. Lett.*, *42*, 9121–9127, doi:10.1002/2015GL065079.

Collinson, G. A., D. O. Kataria, A. J. Coates, S. M. E. Tsang, C. S. Arridge, G. R. Lewis, R. A. Frahm, J. D. Winningham, and S. Barabash (2009), Electron optical study of the Venus Express ASPERA-4 Electron Spectrometer (ELS) top-hat electrostatic analyser, *Meas. Sci. Technol.*, *20*(5), 055,204.

Collinson, G. A., et al. (2012a), Hot flow anomalies at Venus, *J. Geophys. Res.*, *117*, A04204, doi:10.1029/2011JA017277.

Collinson, G. A., L. B. Wilson III, D. G. Sibeck, N. Shane, T. L. Zhang, T. E. Moore, A. J. Coates, and S. Barabash (2012b), Short large-amplitude magnetic structures (SLAMS) at Venus, *J. Geophys. Res.*, *117*, A10221, doi:10.1029/2012JA017838.

Collinson, G. A., et al. (2014), A survey of hot flow anomalies at Venus, *J. Geophys. Res. Space Physics*, *119*, 978–991, doi:10.1002/2013JA018863.

Eastwood, J. P., et al. (2005), Observations of multiple X-line structure in the Earth's magnetotail current sheet: A Cluster case study, *Geophys. Res. Lett.*, *32*, L11105, doi:10.1029/2005GL022509.

Eastwood, J. P., et al. (2008), THEMIS observations of a hot flow anomaly: Solar wind, magnetosheath, and ground-based measurements, *Geophys. Res. Lett.*, *35*, L17S03, doi:10.1029/2008GL033475.

Facskó, G., Z. Németh, G. Erdos, A. Kis, and I. Dandouras (2009), A global study of hot flow anomalies using Cluster multi-spacecraft measurements, *Ann. Geophys.*, *27*, 2057–2076.

Fairfield, D. H. (1969), Bow shock associated waves observed in the far upstream interplanetary medium, *J. Geophys. Res.*, *74*, 3541–3553.

Fairfield, D. H. (1971), Average and unusual locations for the Earth's magnetopause and bow shock, *J. Geophys. Res.*, *76*, 6700–6716.

Greenstadt, E. W., I. M. Green, G. T. Inouye, A. J. Hundhausen, S. J. Bame, and I. B. Strong (1968), Correlated magnetic field and plasma observations of the Earth's bow shock, *J. Geophys. Res.*, *73*, 51–60, doi:10.1029/JA073i001p00051.

Gutynska, O., D. G. Sibeck, and N. Omidi (2015), Magnetosheath plasma structures and their relation to foreshock processes, *J. Geophys. Res. Space Physics*, *120*, 7687–7697, doi:10.1002/2014JA020880.

Halekas, J., E. Taylor, G. Dalton, G. Johnson, D. Curtis, J. McFadden, D. Mitchell, R. Lin, and B. Jakosky (2013), The solar wind ion analyzer for MAVEN, *Space Sci. Rev.*, *195*, 1–27, doi:10.1007/s11214-013-0029-z.

Hellinger, P., and A. Mangeney (1999), Electromagnetic ion beam instabilities: Oblique pulsations, *J. Geophys. Res.*, *104*, 4669–4680.

Hoppe, M. M., and C. T. Russell (1983), Plasma rest frame frequencies and polarizations of the low-frequency upstream waves—ISEE 1 and 2 observations, *J. Geophys. Res.*, *88*, 2021–2027.

Kajdič, P., X. Blanco-Cano, N. Omidi, and C. T. Russell (2011), Multi-spacecraft study of foreshock cavitons upstream of the quasi-parallel bow shock, *Planet. Space. Sci.*, *59*, 705–714, doi:10.1016/j.pss.2011.02.005.

Kajdič, P., X. Blanco-Cano, N. Omidi, K. Meziane, C. T. Russell, J.-A. Sauvaud, I. Dandouras, and B. Lavraud (2013), Statistical study of foreshock cavitons, *Ann. Geophys.*, *31*, 2163–2178, doi:10.5194/angeo-31-2163-2013.

Kovacs, P., G. Facsko, and I. Dandouras (2014), Turbulent dynamics inside the cavity of hot flow anomaly, *Planet. Space Sci.*, *92*, 24–33.

Lucek, E. A., T. S. Horbury, A. Balogh, I. Dandouras, and H. Rème (2004), Cluster observations of hot flow anomalies, *J. Geophys. Res.*, *109*, A06207, doi:10.1029/2003JA010016.

Masters, A., et al. (2008), Cassini encounters with hot flow anomaly-like phenomena at Saturn's bow shock, *Geophys. Res. Lett.*, *35*, L02202, doi:10.1029/2007GL032371.

Masters, A., et al. (2009), Hot flow anomalies at Saturn's bow shock, *J. Geophys. Res.*, *114*, A08217, doi:10.1029/2009JA014112.

Mazelle, C., et al. (2003), Production of gyrating ions from nonlinear wave-particle interaction upstream from the Earth's bow shock: A case study from Cluster-CIS, *Planet. Space. Sci.*, *51*, 785–795.

Meziane, K., et al. (2004), Bow shock specularly reflected ions in the presence of low-frequency electromagnetic waves: A case study, *Ann. Geophys.*, *22*, 2325–2335.

Mitchell, D. L., et al. (2016), The MAVEN solar wind electron analyzer, *Space Sci. Rev.*, *200*, 495–528, doi:10.1007/s11214-015-0232-1.

Ness, N. F., K. W. Behannon, R. P. Lepping, Y. C. Whang, and K. H. Schatten (1974), Magnetic field observations near Venus: Preliminary results from Mariner 10, *Science*, *183*, 1301–1306.

Øieroset, M., D. L. Mitchell, T. D. Phan, R. P. Lin, and M. H. Acuña (2001), Hot diamagnetic cavities upstream of the Martian bow shock, *Geophys. Res. Lett.*, *28*, 887–890.
Omidi, N., H. Zhang, D. Sibeck, and D. Turner (2013), Spontaneous hot flow anomalies at quasi-parallel shocks: 2. Hybrid simulations, *J. Geophys. Res. Space Physics*, *118*, 173–180, doi:10.1029/2012JA018099.
Omidi, N., H. Zhang, C. Chu, D. Sibeck, and D. Turner (2014), Parametric dependencies of spontaneous hot flow anomalies, *J. Geophys. Res. Space Physics*, *119*, 9823–9833, doi:10.1002/2014JA020382.
Omidi, N., J. Berchem, D. Sibeck, and H. Zhang (2016), Impacts of spontaneous hot flow anomalies on the magnetosheath and magnetopause, *J. Geophys. Res. Space Physics*, *121*, 3155–3169, doi:10.1002/2015JA022170.
Omidi, N., G. Collinson, and D. Sibeck (2017), Structure and properties of the foreshock at Venus, *J. Geophys. Res. Space Physics*, doi:10.1002/2017JA024180.
Russell, C. T., R. C. Elphic, and J. A. Slavin (1979), Initial Pioneer Venus magnetic field results—Dayside observations, *Science*, *203*, 745–748.
Scarf, F. L., R. W. Fredricks, L. A. Frank, C. T. Russell, P. J. Coleman Jr., and M. Neugebauer (1970), Direct correlations of large-amplitude waves with suprathermal protons in the upstream solar wind, *J. Geophys. Res.*, *75*, 7316–7322.
Schwartz, S. J. (1995), Hot flow anomalies near the Earth's bow shock, *Adv. Space Res.*, *15*, 107–116.
Schwartz, S. J., G. Paschmann, N. Sckopke, T. M. Bauer, M. Dunlop, A. N. Fazakerley, and M. F. Thomsen (2000), Conditions for the formation of hot flow anomalies at Earth's bow shock, *J. Geophys. Res.*, *105*, 12,639–12,650.
Sibeck, D. G., N. L. Borodkova, G. N. Zastenker, S. A. Romanov, and J.-A. Sauvaud (1998), Gross deformation of the dayside magnetopause, *Geophys. Res. Lett.*, *25*, 453–456.
Sibeck, D. G., et al. (1999), Comprehensive study of the magnetospheric response to a hot flow anomaly, *J. Geophys. Res.*, *104*, 4577–4594.
Slavin, J. A., et al. (1980), The solar wind interaction with Venus—Pioneer Venus observations of bow shock location and structure, *J. Geophys. Res.*, *85*, 7625–7641.
Slavin, J. A., et al. (2009), MESSENGER and Venus Express observations of the solar wind interaction with Venus, *Geophys. Res. Lett.*, *36*, L09106, doi:10.1029/2009GL037876.
Smith, E. J., L. Davis Jr., P. J. Coleman Jr., and C. P. Sonett (1965a), Magnetic measurements near Venus, *J. Geophys. Res.*, *70*, 1571–1586.
Smith, E. J., L. Davis, P. J. Coleman, and D. E. Jones (1965b), Magnetic field measurements near Mars, *Science*, *149*(3689), 1241–1242.
Strangeway, R. J., and G. K. Crawford (1995), Comparison of upstream phenomena at Venus and Earth, *Adv. Space Res.*, *16*, doi:10.1016/0273-1177(95)00219-5.
Thomsen, M. F., V. A. Thomas, D. Winske, J. T. Gosling, M. H. Farris, and C. T. Russell (1993), Observational test of hot flow anomaly formation by the interaction of a magnetic discontinuity with the bow shock, *J. Geophys. Res.*, *98*, 15319–15330, doi:10.1029/93JA00792.
Tjulin, A., E. A. Lucek, and I. Dandouras (2008), Wave activity inside hot flow anomaly cavities, *J. Geophys. Res.*, *113*, A08113, doi:10.1029/2008JA013333.
Tsubouchi, K., and B. Lembège (2004), Full particle simulations of short large-amplitude magnetic structures (SLAMS) in quasi-parallel shocks, *J. Geophys. Res.*, *109*, A02114, doi:10.1029/2003JA010014.
Tsurutani, B. T., and P. Rodriguez (1981), Upstream waves and particles: An overview of ISEE results, *J. Geophys. Res.*, *86*, 4319–4324.
Tsurutani, B. T., E. J. Smith, R. M. Thorne, J. T. Gosling, and H. Matsumoto (1987), Steepened magnetosonic waves at Comet Giacobini-Zinner, *J. Geophys. Res.*, *92*, 11,074–11,082.
Uritsky, V. M., et al. (2014), Active current sheets and candidate hot flow anomalies upstream of Mercury's bow shock, *J. Geophys. Res. Space Physics*, *119*, 853–876, doi:10.1002/2013JA019052.
Vaisberg, O. L., J. H. Waite, L. A. Avanov, V. N. Smirnov, D. L. Dempsey, J. L. Burch, and A. A. Skalsky (1999), HFA-like signatures observed with Interball-tail spacecraft, in *Proceeding of the Solar Wind 9 Conference*, vol. 471, edited by S. T. Suess, G. A. Gary, and S. F. Nerney, pp. 551–554, Am. Inst. of Phys. Conf., College Park, Md.
Vignes, D., et al. (2000), The solar wind interaction with Mars: Locations and shapes of the bow shock and the magnetic pile-up boundary from the observations of the MAG/ER Experiment onboard Mars Global Surveyor, *Geophys. Res. Lett.*, *27*, 49–52, doi:10.1029/1999GL010703.
Wilson, L. B., III, C. A. Cattell, P. J. Kellogg, K. Goetz, K. Kersten, J. C. Kasper, A. Szabo, and K. Meziane (2009), Low-frequency whistler waves and shocklets observed at quasi-perpendicular interplanetary shocks, *J. Geophys. Res.*, *114*, A10106, doi:10.1029/2009JA014376.
Withers, P. (2009), A review of observed variability in the dayside ionosphere of Mars, *Adv. Space Res.*, *44*, 277–307, doi:10.1016/j.asr.2009.04.027.
Zhang, H., D. G. Sibeck, Q.-G. Zong, S. P. Gary, J. P. McFadden, D. Larson, K.-H. Glassmeier, and V. Angelopoulos (2010), Time History of Events and Macroscale Interactions during Substorms observations of a series of hot flow anomaly events, *J. Geophys. Res.*, *115*, A12235, doi:10.1029/2009JA015180.
Zhang, H., D. G. Sibeck, Q.-G. Zong, N. Omidi, D. Turner, and L. B. N. Clausen (2013), Spontaneous hot flow anomalies at quasi-parallel shocks: 1. Observations, *J. Geophys. Res. Space Physics*, *118*, 3357–3363, doi:10.1002/jgra.50376.
Zhang, T. L., et al. (2006), Magnetic field investigation of the Venus plasma environment: Expected new results from Venus Express, *Planet. Space. Sci.*, *54*, 1336–1343.